

# Electrosynthesis and electrochemical characterisation of phenazine polymers for application in biosensors

Madalina M. Barsan, Edilson M. Pinto, Christopher M.A. Brett\*

*Departamento de Química, Universidade de Coimbra, 3004-535 Coimbra, Portugal*

Received 9 July 2007; received in revised form 2 October 2007; accepted 4 October 2007

Available online 12 October 2007

## Abstract

A comparative investigation has been undertaken of the electrosynthesis and electrochemical properties of three different electroactive polymers on carbon film electrode substrates: poly(neutral red) from the phenazine dye neutral red, and poly(methylene green) and poly(methylene blue), from the corresponding phenothiazine dyes. The formation of the radical cation at different potentials and the chemical structures of the monomers both influence the electropolymerisation process of the three polyaromatic dyes. Of the three, poly(neutral red) is shown to have the best adhesion at carbon film electrodes. The influence of the electrolyte and pH on film growth and on electrochemical properties was investigated. The formal potential decreased linearly with increase in pH, in the pH range from 1 to 7 for all three polymers. The modified electrodes were also characterised by electrochemical impedance spectroscopy. The bulk and interfacial characteristics of the two phenothiazine polymers were similar and oxygen-dependent, but different to those of the phenazine polymer, poly(neutral red), which were not significantly influenced by the presence of oxygen in solution. Perspectives for use in electrochemical biosensors are indicated.

© 2007 Elsevier Ltd. All rights reserved.

*Keywords:* Poly(neutral red); Poly(methylene green); Poly(methylene blue); Electropolymerisation; Electroactive polymers

## 1. Introduction

Electropolymerisation is a powerful tool in the development of modified electrodes; electropolymerised materials possess some unique properties, which the corresponding monomers do not have and can be immobilized on electrode surfaces. In the past few years, much work has been carried out on electrosynthesised polymers, particularly on polyaniline and polypyrrole due to their practical application in the construction of “micro-miniaturized” sensing surfaces [1]. However, when it comes to building an enzyme electrode with these polymers, it was found that their electrical conductivity is rather low in the potential range needed for the enzyme reaction, giving rise to a low catalytic current [2]. One way to overcome this problem is to prepare conducting films by electropolymerisation of a monomer, which is itself a redox-active compound.

Surface-modified electrodes based on the electropolymerisation of viologen [3] and several phenazine, phenoxazine and phenothiazine derivatives have been reported in the literature [4,5].

Methylene blue was extensively used as mediator in a NAD-dependent dehydrogenase biosensor, since it is known to have good electrocatalytic properties with respect to NADH oxidation [6,7]. A sensor for haemoglobin based on poly(methylene blue) (PMB) electrodeposited on glassy carbon has also been reported [8]. Methylene green (MG) was mostly employed for the construction of hydrogen peroxide biosensors based on immobilization of horseradish peroxidase in an electropolymerised MG film of poly(methylene green) (PMG) on a glassy carbon electrode [9], co-immobilization of MG with horseradish peroxidase [10] or by incorporating MG in a Nafion membrane [11] and, as a sensor, it was used for the detection of theophylline [12].

Poly(neutral red) (PNR) has been extensively used as mediator for the construction of various biosensor assemblies, for glucose, pyruvate and alcohol detection [13,14]. A biosensor was developed for use in flow analysis for glucose monitoring, containing the enzyme entrapped in a sol-gel layer on a PNR-modified carbon film electrode [15]. Recently, a study of the characterisation of PNR-modified carbon film electrodes and their application as redox mediator for biosensors was published [16].

One of the drawbacks of these two electron–proton type mediators is the dependence of their formal potential on pH. In

\* Corresponding author. Tel.: +351 239 835295; fax: +351 239 835295.  
E-mail address: [brett@ci.uc.pt](mailto:brett@ci.uc.pt) (C.M.A. Brett).

order to overcome this problem, many investigations have been focused on finding new electrode materials and ways to immobilize the organic dyes so that the formal potential is invariant with change in pH. Some studies have shown that when various phenoxazine and phenothiazine-type mediators are immobilized onto zirconium phosphate [17,18], or incorporated into modernite type zeolites [19], their  $E^0$  values remain constant with pH.

Electrochemical impedance spectroscopy (EIS) has previously been little used in characterising these polymer films [20–23], but can give valuable information about the phenomena involved in the overall redox processes and about the bulk and interfacial characteristics of the films.

The aim of this work is to present a comparative investigation into the electropolymerisation and electrochemical properties of the three different electroactive polymers poly(neutral red) (PNR) from the phenazine dye neutral red, and poly(methylene green) (PMG) and poly(methylene blue) (PMB) made from the corresponding phenothiazine dyes. The electrochemical behaviour was investigated by cyclic voltammetry and by EIS, with a view to understanding the advantages of each of the polymers as redox mediators in electrochemical enzyme biosensors.

## 2. Experimental

### 2.1. Reagents and buffer electrolyte solutions

Neutral red monomer (NR), 65% dye content and methylene blue monomer (MB) were from Aldrich (Germany) and methylene green zinc chloride salt (MG) was from Fluka (Switzerland). The chemical structures of the monomers are presented in Fig. 1.

The buffer solution used for the electropolymerisation of NR was 0.025 M potassium phosphate saline (KPBS) pH 5.5 prepared from potassium hydrogen phosphate (Riedel-deHaën, Germany) and di-potassium hydrogen phosphate 3-hydrate (Panreac, Spain) with the addition of 0.1 M potassium chloride (Fluka, Switzerland). For the electropolymerisation of MG, six different buffer solutions were used, in a pH range from 5.5 up to 9.3. The KPBS solutions, pH 5.5 and 7.0, were prepared as described above with addition of 0.1 M KCl or 0.1 M potassium nitrate (Riedel-deHaën, Germany) and the 0.025 M sodium tetraborate saline solutions were prepared from disodium tetraborate 10-hydrate (Merck, Germany) and sodium hydroxide (Riedel-de-Haën, Germany) with addition of 0.1 M KCl (sodium tetraborate saline pH 9.33) and with addition of 0.1 M  $\text{KNO}_3$  (sodium borate saline pH 9.2). Four buffer solutions were used for the electropolymerisation of MB: 0.1 M sodium phosphate saline (NaPBS) prepared from di-sodium hydrogen phosphate 2-hydrate (Riedel-deHaën, Germany) and sodium phosphate monobasic monohydrate (Sigma–Aldrich, Germany) with the addition of 0.05 M sodium chloride (Riedel-deHaën, Germany) (NaPBS pH 8.1) or with the addition of 0.05 M sodium sulphate (Merck, Germany) (NaPBS pH 8.2).

The concentration of the three dyes dissolved in the buffer solutions was always 1 mM.

The electrolytes used for the characterisation of the phenazine and phenothiazine modified electrodes were 0.1 M KCl, 0.1 M NaCl, 0.1 M lithium chloride (Panreac, Spain), and another seven buffer solutions having the pH in the range of 1.06 up to 7.05. The buffer solutions with pH 1.06 and 2.07 were prepared by mixing KCl with hydrochloric acid (37% Riedel-deHaën, Germany) and the buffer solutions pH 3.4 and 4.5 were prepared

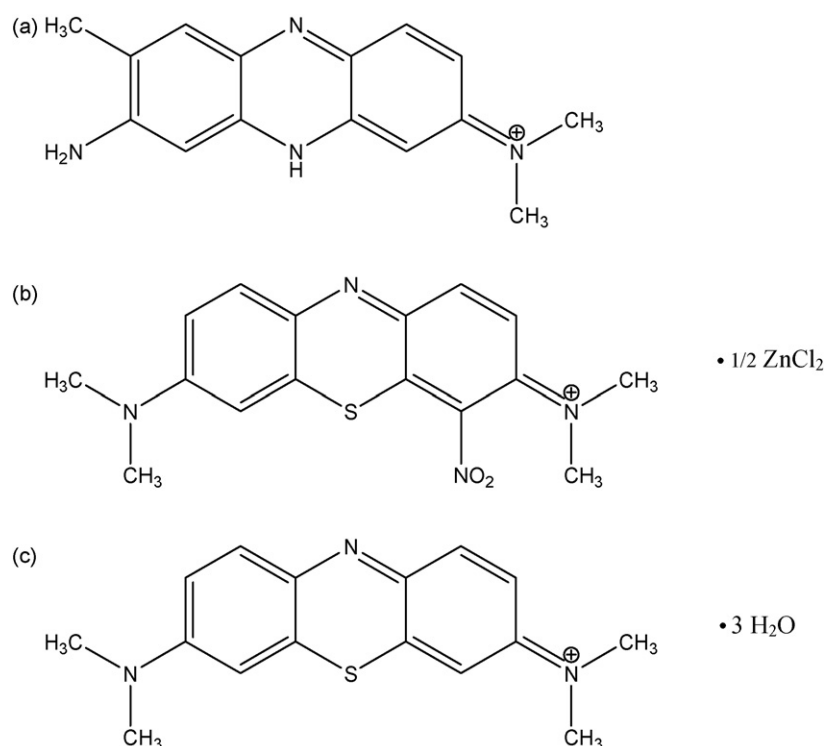


Fig. 1. Chemical structures of the monomers (a) neutral red, (b) methylene green zinc chloride salt and (c) methylene blue 3-hydrate.

by mixing sodium acetate with acetic acid, both from Riedel-deHaën, Germany. The other three buffer solutions used were 0.025 M KPBS + 0.1 M KCl with pH 5.5, 6.0 and 7.0.

Millipore Milli-Q nanopure water (resistivity  $\geq 18 \text{ M}\Omega \text{ cm}$ ) and analytical reagents were used for preparation of all solutions. Experiments were performed at room temperature,  $25 \pm 1 \text{ }^\circ\text{C}$ .

## 2.2. Instrumentation

Carbon film cylindrical electrodes were made from carbon film electrical resistors ( $2 \Omega$  resistance) of length 6 mm and diameter 1.5 mm, as described elsewhere, with an exposed surface area of  $\sim 0.20 \text{ cm}^2$  [24]. A three-electrode electrochemical cell of volume  $10 \text{ cm}^3$  was used, containing the modified carbon film electrode as working electrode, a platinum foil counter electrode and a saturated calomel electrode (SCE) as reference.

All electrochemical measurements were performed using a computer-controlled  $\mu$ -Autolab Type II potentiostat-galvanostat running with GPES (General Purpose Electrochemical System) for Windows version 4.9, software (EcoChemie, Utrecht, Netherlands).

The electrochemical impedance measurements were done on a PGSTAT 30 potentiostat-galvanostat with Frequency Response Analyser (FRA2) module controlled by FRA software version 4.9 (EcoChemie, Utrecht, Netherlands). A rms perturbation of 10 mV was applied over the frequency range 65 kHz to 0.01 Hz with 10 frequency values per decade. The spectra were recorded at the potentials of  $-0.6$ ,  $-0.3$ ,  $0.0$  and  $+0.3 \text{ V}$  versus SCE.

The pH-measurements were carried out with a CRISON 2001 micro pH-meter at room temperature.

## 2.3. Preparation of polymer-modified electrodes

Before performing the electropolymerisations, the electrodes were electrochemically pretreated, first by applying a fixed potential of  $+0.9 \text{ V}$  versus SCE during 240 s, followed by potential cycling between  $-1.0$  and  $+1.0 \text{ V}$  versus SCE at a scan rate of  $100 \text{ mV s}^{-1}$ , until a stable voltammogram was obtained. The electrolytes used for pretreatment were always the same as those used for the electropolymerisation of the dye monomer.

All polymers were prepared as films on the carbon film electrode substrate by cyclic voltammetry from the buffer solutions described in Section 2.1, containing 1 mM monomer, at a scan rate of  $50 \text{ mV s}^{-1}$ . The potential was cycled in different ranges, between  $-1.0$  and  $+1.0 \text{ V}$  versus SCE for 15 cycles for making PNR films, according to procedures previously optimised in [13,15,25],  $-0.5$  and  $+1.0 \text{ V}$  versus SCE during 30 cycles for PMG and for PMB films between  $-0.75$  and  $+1.0 \text{ V}$  versus SCE for 30 cycles.

## 3. Results and discussion

### 3.1. Electropolymerisation of the monomer dyes

The preparation of the polymer films was carried out as described in Section 2. For both PMG and PMB films, different buffers of different pH were used to prepare the solutions used

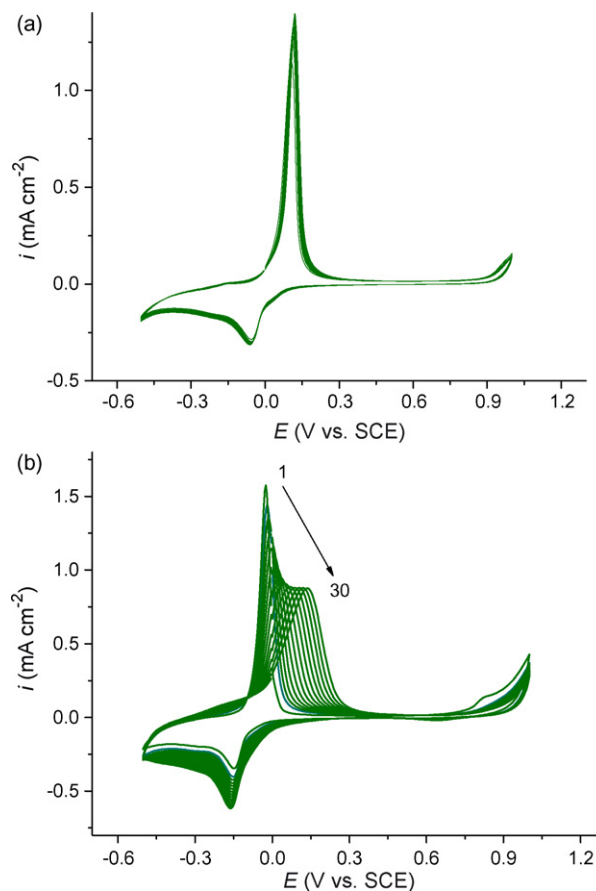


Fig. 2. Electropolymerisation of MG from a solution containing 1 mM MG monomer in (a) 0.025 M KPBS + 0.1 M KCl pH 5.5 and (b) 0.025 M  $\text{Na}_2\text{B}_4\text{O}_7$  + 0.1 M  $\text{KNO}_3$  pH 9.2; 30 cycles between  $-0.5$  and  $+1.0 \text{ V}$  vs. SCE at scan rate  $50 \text{ mV s}^{-1}$ .

for electropolymerisation of the monomers at the carbon film electrodes. Since optimisation of the preparation procedure of PNR films on carbon film electrodes was already done [13,16], we only report here 0.025 M KPBS + 0.1 M  $\text{KNO}_3$  pH 5.5, found to be the appropriate one for PNR preparation.

It was observed that for both phenothiazine dyes, film growth is facilitated when alkaline buffer solutions are used. Fig. 2 shows the electropolymerisation of MG from 1 mM monomer in buffer solutions at pH 5.5 and pH 9.3. While in the first case, Fig. 2a, the peak potential and peak current values did not change significantly during the electropolymerisation, when alkaline solution is used, Fig. 2b, a different voltammetric profile is recorded. The initial signal due to the monomer, at  $-0.045 \text{ V}$  versus SCE, decreases and the anodic peak potential shifts toward more positive values, reaching  $+0.058 \text{ V}$  versus SCE in the 30th cycle, and which corresponds to the polymer. Also, for both 0.025 M KPBS buffer solutions, that at pH 7.0 containing 0.1 M  $\text{KNO}_3$  or 0.1 M KCl and for the other at pH 5.5 containing 0.025 M KPBS buffer + 0.1 M  $\text{KNO}_3$ , the same voltammetric profiles as in Fig. 3a, were observed.

Methylene blue electropolymerised better at carbon film electrode substrates than did methylene green. It seems that the presence of the  $-\text{NO}_2$  group in MG (see Fig. 1) hinders the electropolymerisation process to a small extent. Fig. 3 shows the

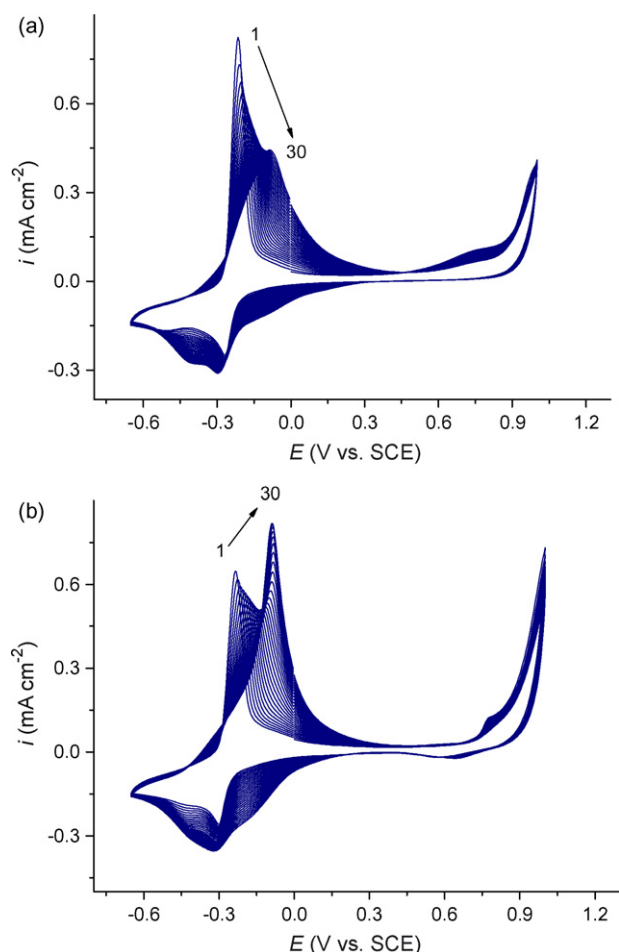


Fig. 3. Electropolymerisation of MB from a solution containing 1 mM MB monomer in (a) 0.1 M NaPBS + 0.05 M NaCl pH 8.1 and (b) 0.025 M  $\text{Na}_2\text{B}_4\text{O}_7$  + 0.1 M NaOH + 0.1 M  $\text{Na}_2\text{SO}_4$ ; 30 cycles between  $-0.65$  and  $+1.0$  V vs. SCE at scan rate  $50 \text{ mV s}^{-1}$ .

electropolymerisation of MB. As in the case of PMG film formation, the same voltammetric profile of the electropolymerisation process was observed in 0.1 M NaPBS + 0.05 M NaCl pH 8.1, but for the same pH with buffer containing  $\text{Na}_2\text{SO}_4$  supporting electrolyte instead of NaCl, the polymer growth is much more

evident, Fig. 3a, suggesting that  $\text{SO}_4^{2-}$  anions have a catalytic effect on the electropolymerisation of MB. The film growth was even more notable when 0.025 M  $\text{Na}_2\text{B}_4\text{O}_7$  + 0.1 M NaOH + 0.1 M  $\text{Na}_2\text{SO}_4$  was used (Fig. 3b). The initial anodic signal due to the monomer, at  $-0.235$  V versus SCE, decreases and peaks corresponding to the polymer increase in size with successive cycles and the anodic peak potential shifts toward more positive values up to  $-0.087$  V versus SCE in the 30th cycle.

The quantity of electroactive polymer deposited by electropolymerisation from each buffer was calculated using Faraday's law, considering that the two electrons are involved in all redox reactions [6]. The charge was calculated for each type of poly(phenothiazine)-modified electrode from cyclic voltammograms recorded in 0.1 M KCl electrolyte. For the PMG films deposited from the KPBS buffers at pH 5.5, the calculation was not made, since it was observed that the film was poorly adherent and washed from the surface after only several immersions of the sensor in the electrolyte solution. The results obtained are presented in Table 1. As expected from the electropolymerisation voltammogram profiles, thicker PMB and PMG films were formed when alkaline solutions were used for the polymerisation. Moreover, when the supporting electrolyte contains  $\text{SO}_4^{2-}$  or  $\text{NO}_3^-$ , the polymer films are even thicker, suggesting that these anions catalyse the deposition process. The catalytic effect of the nitrate ions was already observed in the case of MB electropolymerisation [26].

Regarding the formation of PNR, the peak potential values of the NR monomer and polymer are the same. Polymer peaks increase in height with film growth especially in the first 10 cycles (Fig. 4).

For all three polymers, the polymerisation reaction begins with adsorption of the monomer onto the carbon film electrode and formation of the cation-radical species at high positive potentials. Since the chemical structures of the polymer precursors are different (see Fig. 1), the whole polymerisation process will differ from one species to another. It was observed that the PMG film is the first to dissolve from the electrode surface after several uses.

When the monomer has a primary amino group as a ring substituent, as in the case of NR, the cation-radical species formed

Table 1  
Polymer oxidation charge and corresponding number of moles of monomer from cyclic voltammograms recorded at PMG PMB and PNR-modified electrode immersed in 0.1 M KCl, potential range  $-1.0$  to  $1.0$  V vs. SCE, scan rate  $50 \text{ mV s}^{-1}$

Polymer	Buffer used for polymerisation	$q_i$ ( $\text{mC cm}^{-2}$ )	Amount of monomer ( $\text{nmol cm}^{-2}$ )
<b>PMG</b>			
PMG <sub>1</sub>	0.025 M KPBS + 0.1 M KCl pH 7.0	0.81	4.0
PMG <sub>2</sub>	0.025 M KPBS + 0.1 M $\text{KNO}_3$ pH 7.0	1.00	5.0
PMG <sub>3</sub>	0.025 M borate + 0.1 M $\text{KNO}_3$ pH 9.2	1.70	9.0
PMG <sub>4</sub>	0.025 M borate + 0.1 M KCl pH 9.33	1.14	6.0
<b>PMB</b>			
PMB <sub>1</sub>	0.1 M NaPBS + 0.05 M NaCl pH 8.1	1.18	6.0
PMB <sub>2</sub>	0.1 M NaPBS + 0.1 M $\text{Na}_2\text{SO}_4$ pH 8.2	1.28	6.5
PMB <sub>3</sub>	0.025 M borate + 0.1 M $\text{Na}_2\text{SO}_4$ pH 9.2	1.99	10.5
PMB <sub>4</sub>	0.025 M borate + 0.1 M NaCl pH 9.25	1.65	8.5
<b>PNR</b>			
PNR	0.025 M KPBS + 0.1 M $\text{KNO}_3$ pH 5.5	2.44	12.5

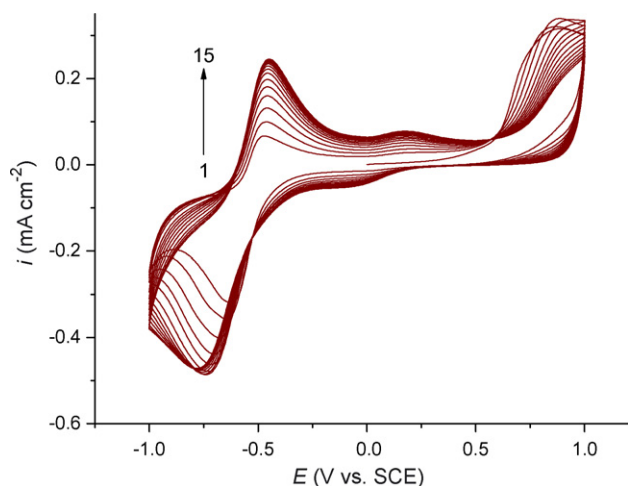


Fig. 4. Electropolymerisation of NR from a solution containing 1 mM NR monomer in 0.025 M KPBS + 0.1 M  $\text{KNO}_3$  pH 5.5; 15 cycles between  $-1.0$  and  $+1.0$  V vs. SCE at scan rate  $50 \text{ mV s}^{-1}$ .

at  $\approx +0.8$  V versus SCE will be activated in the free ortho position with respect to the amino group in the aromatic ring. In this way, the polymer is probably composed of phenazine units linked through a secondary amino moiety. A proposed structure of the neutral red dimer is presented in Fig. 5a. In the case of MB and MG phenothiazine dyes, where the monomers contain two tertiary amino groups, the cation-radical species are formed at much more positive potentials, closer to the potential corresponding to oxygen evolution. Probably in this case, before forming the cation-radical species, at least one of the tertiary amino substituents should be oxidized in a mechanism involving hydroperoxides. These reactive anions may afterwards attack one of the methyl groups of the tertiary amino group bound to the aromatic ring, with release of formaldehyde. It has been reported that FTIR spectra of PMB present carbonyl signals [27], which

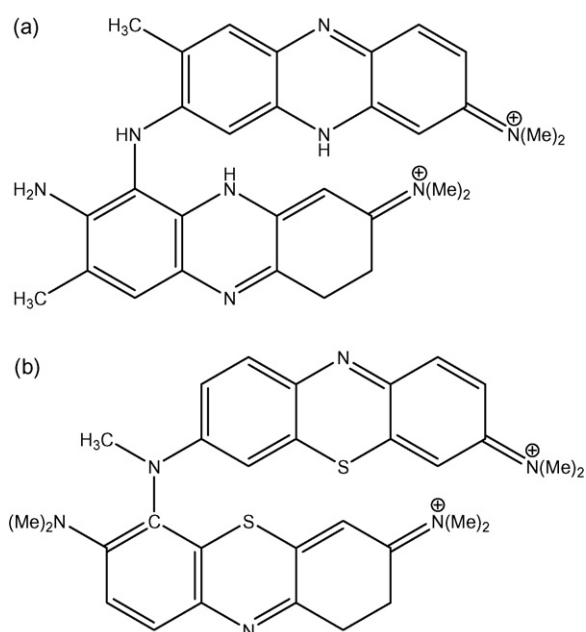


Fig. 5. Proposed structures for (a) NR dimer and (b) MB dimer.

indicates that the phenothiazine monomer units are probably linked through a nitrogen atom, see Fig. 5b.

### 3.2. Cyclic voltammetry characterisation of the PNR-, PMG- and PMB-modified electrodes

The designation of the different types of phenothiazine polymer film electrodeposited on carbon film electrodes from the different buffers will be further referred to below in the way presented in Table 1.

#### 3.2.1. Dependence on scan rate

Cyclic voltammograms at different scan rates, from 10 to  $200 \text{ mV s}^{-1}$ , were recorded at  $\text{PMB}_3$  and  $\text{PMG}_3$  as well as at PNR, and are shown in Fig. 6. In all cases, the voltammogram shape is affected by the scan rate and the peak currents, both anodic and cathodic, depend linearly on the square root of the scan rate over the whole scan rate range examined, see Fig. 7. These results imply diffusion-controlled processes [28] and are similar to those reported in [29,30]. In this particular case, the redox process is controlled by diffusion of the electrolyte counterions through the polymer film, which plays an important role in maintaining electroneutrality on the electrode surface.

In the case of PNR (Fig. 7a) the slope of the curve  $I_{\text{pc}}$  versus  $\nu^{1/2}$  is slightly greater than that corresponding to the oxidation process, meaning that the reduction process occurs with a higher electron transfer rate.

The different values of the slopes in the plots in Figs. 7b and c, for both anodic and cathodic currents of  $\text{PMB}_3$  and  $\text{PMG}_3$ , indicate a difference in the diffusion rate for the  $\text{PMB}_3$  and  $\text{PMG}_3$  modified electrodes. In the case of  $\text{PMB}_3$ , as can be seen in Fig. 6c, the peak separation  $\Delta E_{\text{p}} = E_{\text{pa}} - E_{\text{pc}}$  increases at higher scan rates. This is an indication that the kinetics of electron transfer is less fast than for PNR and  $\text{PMG}_3$ .

For all the phenothiazine films, deposited from the other buffers, the same linear relationship between the peak current and the square root of the scan rate was obtained. In both cases, the  $\text{PMG}_3$  and  $\text{PMB}_3$  films showed a faster electron transfer rate than the other films deposited from buffers which did not contain  $\text{NO}_3^-$  or  $\text{SO}_4^{2-}$  ions, having the higher slopes of  $4.25 \mu\text{A} (\text{mV s}^{-1})^{-1/2}$  and  $4.37 \mu\text{A} (\text{mV s}^{-1})^{-1/2}$ , respectively, compared with 2.31 ( $\text{PMG}_1$ ), 2.93 ( $\text{PMG}_2$ ), 1.92 ( $\text{PMG}_4$ ), 3.36 ( $\text{PMB}_1$ ), 3.4 ( $\text{PMB}_2$ ) and 3.54 ( $\text{PMB}_4$ )  $\mu\text{A} (\text{mV s}^{-1})^{-1/2}$  (anodic peak currents). The same was observed in the case of cathodic peak currents. These slopes correspond to diffusion coefficients of the order of  $10^{-10} \text{ cm}^2 \text{ s}^{-1}$ .

In the case of PMG and PMB, since counterion diffusion through the polymer film is the rate-determining step of the overall redox process, the expulsion of the counterion, which occurs during oxidation of the polymer, is faster than its diffusion into the polymer film. On the contrary, in the case of PNR, counterion diffusion into the polymer film is faster.

#### 3.2.2. The effect of the counter ion of the supporting electrolyte

As was shown above, the diffusion of the electrolyte counterion to/from the polymer film is the rate-determining step of

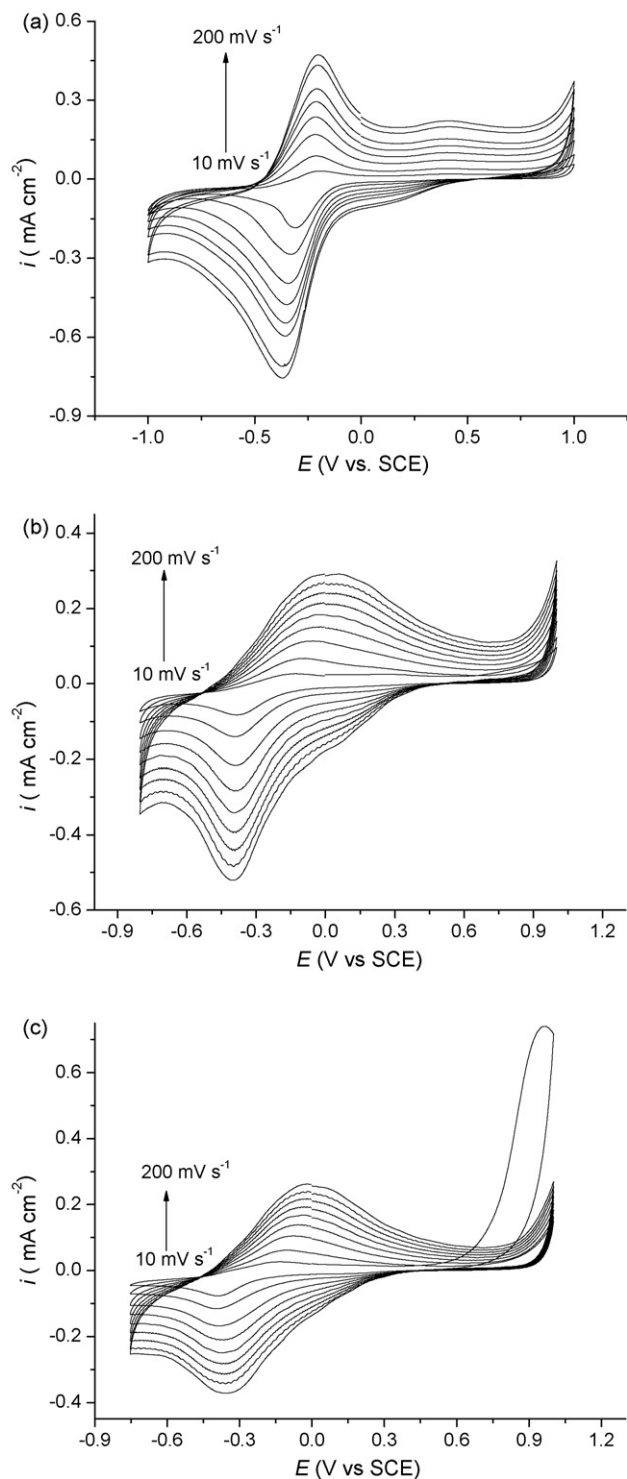


Fig. 6. Cyclic voltammograms at (a) PNR, (b) PMG<sub>3</sub> and (c) PMB<sub>3</sub> in 0.1 M KCl solution at different scan rates, from 10 to 200 mV s<sup>-1</sup>.

the redox process. Since this plays an important role, a study was made of how the electrolytes containing different cations influence the electrochemical properties of the modified electrodes. The results are presented in Table 2. The reduction of the polymer is coupled to the movement of electrolyte cations from the solution into the polymer matrix, to compensate the change in charge, so that cation movement immediately follows

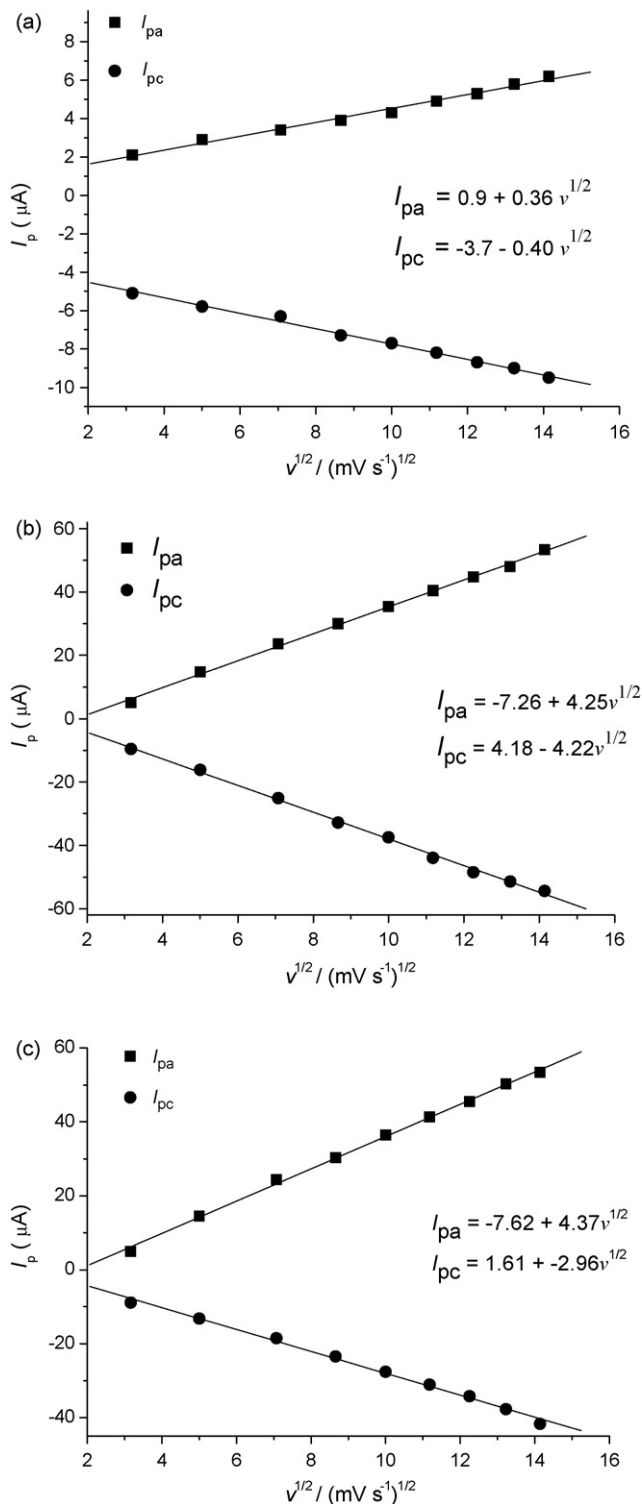


Fig. 7. Plots of peak vs. square root of scan rate for (a) PNR (b) PMG<sub>3</sub> and (c) PMB<sub>3</sub>, calculated from the cyclic voltammograms shown in Fig. 6.

the electroreduction step. In the case of electrolytes with a large hydrated cation radius such as Li<sup>+</sup>, the small current and charge passed during the redox process makes its diffusion through the polymer network more difficult. This was also observed at an electrode containing the MB dye monomer incorporated into a modernite type zeolite, in this case diffusion being through the

Table 2

Midpoint potentials and peak currents for PMG<sub>3</sub>, PMB<sub>3</sub> and PNR-modified electrodes from cyclic voltammograms in various chloride electrolyte solutions, concentration: 0.1 M; scan rate 50 mV s<sup>-1</sup>

Polymer	Electrolyte	$E_m$ (mV) vs. SCE	$I_{pa}$ ( $\mu\text{A cm}^{-2}$ )	$I_{pc}$ ( $\mu\text{A cm}^{-2}$ )
PNR	LiCl	-770	51.5	-24.0
	NaCl	-773	90.0	-30.5
	KCl	-772	95.0	-31.5
PMG <sub>3</sub>	LiCl	-269	50.0	-50.5
	NaCl	-268	60.0	-67.5
	KCl	-267	64.5	-67.5
PMB <sub>3</sub>	LiCl	-312	50.5	-16.5
	NaCl	-311	64.5	-34.5
	KCl	-309	66.0	-36.5

zeolite pores [19]. For electrolytes containing Na<sup>+</sup> and K<sup>+</sup> as cations, no significant differences between the recorded peak currents were observed, even though their hydrated ionic radii are different. This is important, since it is intended that these polymer films will play the role of mediators in a biosensor assembly, where measurements are required to be made in the presence of Na<sup>+</sup> ions.

It should also be noted that the electrolyte type does not have a significant influence on midpoint potential values, being  $-268 \pm 1$  mV in the case of PMG<sub>3</sub>,  $-311 \pm 1$  mV for PMB<sub>3</sub> and  $-772 \pm 2$  mV versus SCE for PNR, suggesting that any effects influence the anodic and cathodic processes equally.

### 3.2.3. The effect of solution pH

One of the major drawbacks of the polyaromatic quinoid-type mediators, being redox species of two electron-proton acceptors/donors, is the dependence of their midpoint potential  $E_m$  on the solution pH. In contrast, the mediators that have a metal ion as redox centre are only electron acceptors/donors, in this way having a midpoint potential which has no pH dependence [31]. It has been found that when phenazine dyes are in solution or chemically adsorbed at electrode surfaces, they possess a midpoint potential which is highly pH-dependent [32,33]. However, recent findings have shown that when various phenoxazine and phenothiazine-type mediators are immobilized onto zirconium phosphate [18] or onto zeolite [19], their formal potential values remain invariant with pH. It was therefore necessary to investigate the variation of midpoint potential with pH for the electropolymerised dyes, since this influences the applied potential at which the redox-mediated biosensors can be used.

In order to determine the midpoint potential value, cyclic voltammograms were recorded at PNR-, PMG- and PMB-modified electrodes at 50 mV s<sup>-1</sup> scan rate in buffer solutions in the pH range between 1 and 7. The midpoint potential  $E_m$  was calculated as the average of the anodic and cathodic peak potentials ( $E_m = (E_{pa} + E_{pc})/2$ ) and was used as an approximation of the formal potential  $E^{0'}$ . It was found that the  $E^{0'}$  values decrease linearly with increase in buffer solution pH, see Fig. 8, according to the equations:  $E_{PNR}^{0'} = -182 - 63\text{pH mV}$ ,  $E_{PMG_3}^{0'} = 279 - 54\text{pH mV}$  and  $E_{PMB_3}^{0'} = 254 - 51\text{pH mV}$  versus SCE, respectively. The values of the slopes of both  $E_{pa}$  and

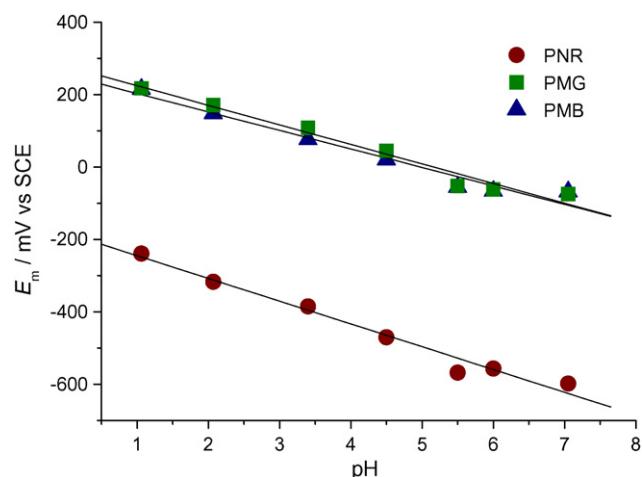


Fig. 8. The influence of pH on the midpoint potential for PNR, PMG<sub>3</sub> and PMB<sub>3</sub>, calculated from cyclic voltammograms recorded at 50 mV s<sup>-1</sup> in the potential range  $-1.0$  to  $+1.0$  V vs. SCE.

$E_{pc}$  versus pH plots for PNR-, PMG- and PMB-modified electrodes, see Table 3, show that in the redox process equal numbers of electrons and protons are involved.

### 3.3. Characterisation of the polymers by EIS

The interfacial characteristics of the PNR-, PMG- and PMB-modified carbon film electrodes were studied by EIS. The experiments were carried out at applied potentials of  $-0.6$ ,  $-0.3$ ,  $0.0$  and  $+0.3$  V versus SCE, chosen to be negative of, coincident with and positive of the oxidation and reduction peaks in the cyclic voltammograms. The spectra are shown in Fig. 9, recorded in the presence and absence of oxygen, for reasons that will be described below.

The spectra recorded in 0.1 M NaPBS + 0.05 M NaCl pH 7 buffer solution, indicate that the overall redox process is controlled by diffusion at low frequency. It was already suggested above in the voltammetric characterisation of the polymers, that the diffusion of the counterion through the polymer film is the rate-determining step of the overall process. Since the diffusion process observed in the impedance spectra could be associated with O<sub>2</sub> diffusion through the polymer film, experiments were also done in deoxygenated buffer solutions.

The equivalent circuit proposed to fit the EIS results, is the same as that used in [21,22], for surfaces covered by electroactive polymers. The equivalent circuit, shown in Fig. 10, consists of the cell resistance,  $R_{\Omega}$ , in series with  $C_f$  and  $R_f$  in parallel, representing the capacitance and the resistance of the film,

Table 3

Slopes of the plots of anodic and cathodic peak potentials ( $E_{pa}$  and  $E_{pc}$ ) vs. pH in the pH range 1.0–6.0, calculated from cyclic voltammograms recorded in the potential range  $-1.0$  to  $+1.0$  V vs. SCE, scan rate 50 mV s<sup>-1</sup>

Polymer	$E_{pa}$ (pH mV/pH unit)	$E_{pc}$ (pH mV/pH unit)
PNR	-48.0	-79.1
PMG <sub>3</sub>	-55.3	-60.1
PMB <sub>3</sub>	-59.2	-57.1

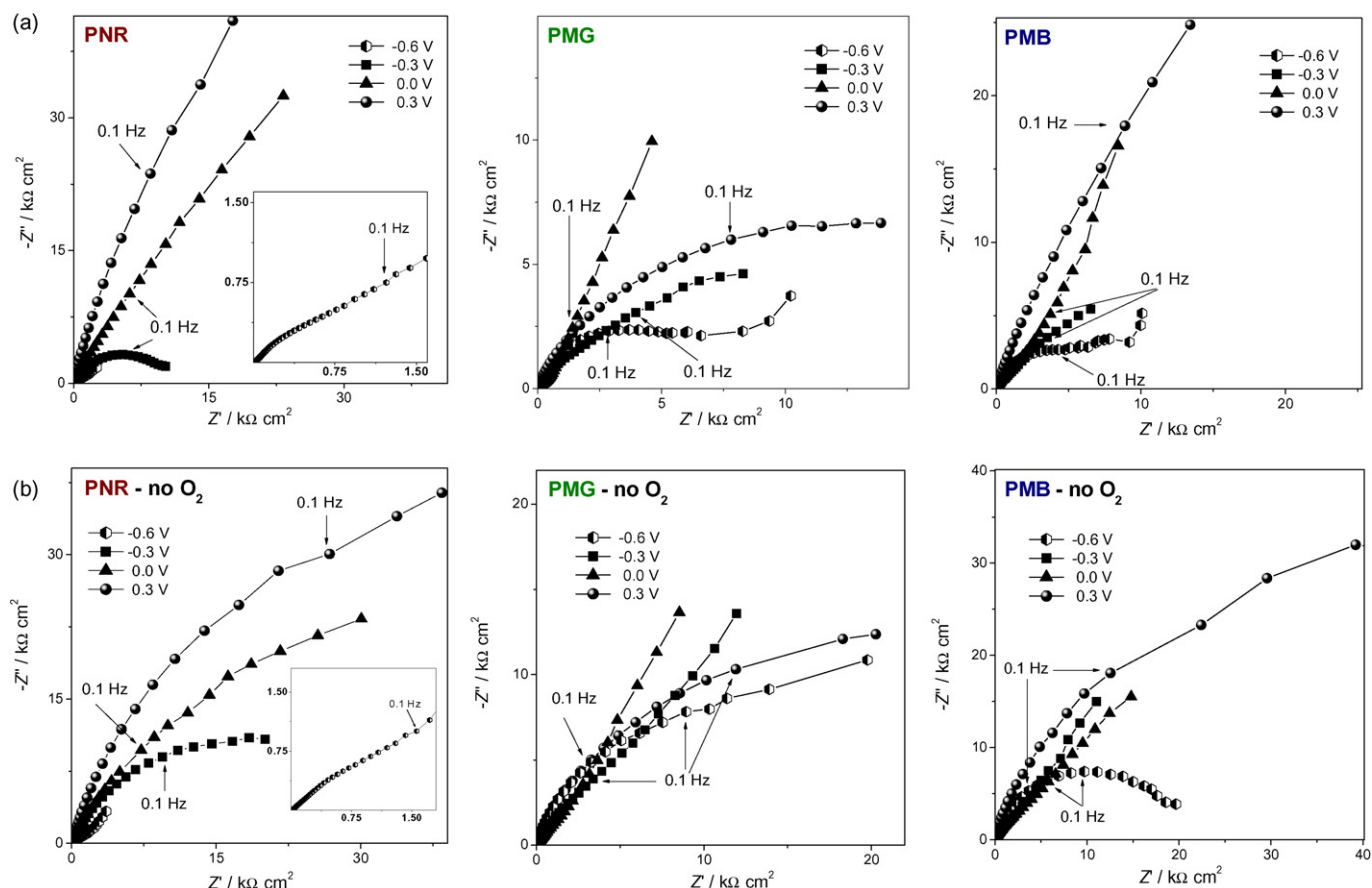


Fig. 9. Complex plane impedance plots recorded in 0.1 M NaPBS + 0.05 M NaCl pH 7 buffer solution, at  $-0.6$ ,  $-0.3$ ,  $0.0$  and  $+0.3$  V vs. SCE at PNR; PMG and PMB (a) in the presence of oxygen and (b) in the absence of oxygen.

respectively. The polymer/solution interface is represented by a mass transport finite-diffusion Warburg element  $Z_W$ , in series with the charge transfer resistance  $R_{ct}$ , in parallel with a constant phase element  $CPE = \{(C_f i \omega)^\alpha\}^{-1}$ , representing the interfacial charge separation, modelled as a non-ideal capacitor, owing to the porosity of the polymer films, and the exponent  $\alpha$  has a value around 0.75.

Table 4 contains the values of  $C_f$  and  $R_f$ , calculated by equivalent circuit fitting. The PNR film presented higher polymer film resistance than that of PMG and PMB films, over the whole potential range. The biggest difference between film resistance values are observed at  $-0.3$  and  $0.0$  V versus SCE, where both PMG and PMB are more conductive, since this corresponds to the potential region where the oxidation and reduction of the polymer occurs. Because of the differences in the recorded spec-

tra, the results will be presented and discussed individually for each polymer film.

The impedance spectra recorded at PNR-modified electrodes in the presence of oxygen are shown in Fig. 9a. The shape, at

Table 4

Values of  $R_f$  and  $C_f$  from fitting of the impedance spectra in Fig. 9, in the presence and absence of  $O_2$ , at PNR-, PMG- and PMB-modified carbon film electrodes

$E$ (V) vs. SCE	Presence of $O_2$		Absence of $O_2$	
	$R_f$ ( $k\Omega cm^2$ )	$C_f$ ( $mF cm^{-2}$ )	$R_f$ ( $k\Omega cm^2$ )	$C_f$ ( $mF cm^{-2}$ )
<b>PNR</b>				
$-0.6$	1.85	0.28	3.40	0.17
$-0.3$	2.25	0.26	4.09	0.11
$0.0$	2.29	0.22	4.37	0.13
$+0.3$	16.7	0.05	12.8	0.01
<b>PMG</b>				
$-0.6$	0.89	0.14	7.63	0.05
$-0.3$	0.59	0.23	3.31	0.19
$0.0$	0.26	0.27	1.28	0.30
$+0.3$	1.63	0.08	18.5	0.01
<b>PMB</b>				
$-0.6$	3.78	0.07	8.56	0.05
$-0.3$	1.19	0.38	2.32	0.23
$0.0$	2.42	0.17	3.28	0.15
$+0.3$	9.57	0.06	16.7	0.04

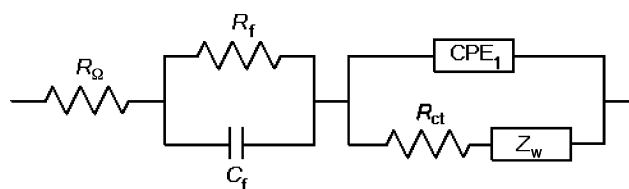


Fig. 10. Equivalent circuit used for fitting of electrochemical impedance spectra. See text for meaning of symbols.

–0.6 V versus SCE, is a semicircle at high frequencies followed by an almost straight line at lower frequencies. This indicates a second process, probably diffusion through the polymer matrix [23]. Since the diffusion of the counterion is correlated with polymer reduction, the same tendency was also observed at –0.3 V versus SCE, with the difference that the first semicircle is followed by a second smaller one. The fact that the straight line was replaced with a semicircle is because at this potential, the oxidation of the PNR polymer occurs. Oxidation leads to a less conductive film, as can be seen by the increase in the  $R_f$  values from 0.10 to 2.25  $\text{k}\Omega\text{ cm}^2$  with  $C_f$  decreasing from 0.83 to 0.26  $\text{mF cm}^{-2}$  on changing the applied potential from –0.6 V to –0.3 V versus SCE (see Table 4).

At more positive potentials, the second process is no longer observed as diffusional: the low frequency straight line at 0.0 V become semicircular at +0.3 V versus SCE. The film resistance continues to increase, reaching a maximum value of 16.7  $\text{k}\Omega\text{ cm}^2$  at +0.3 V versus SCE and a minimum capacitance of 0.05  $\text{mF cm}^{-2}$ .

Comparing spectra in the presence and absence of oxygen, Fig. 9b, differences are more noticeable at 0.0 and 0.3 V versus SCE. In these cases, the curve profile shows greater evidence of mass transport control at low frequencies. At negative potentials the curves maintain the same profile but with higher impedance values. In the absence of oxygen, the film resistances are higher, except at +0.3 V versus SCE, where the film resistance is significantly lower than that calculated in the presence of oxygen. This is the potential corresponding to a small oxidation peak in the cyclic voltammograms, and it may be that the intermediate formed is more stable in the absence of oxygen contributing to the lower resistance observed.

In the case of PMG, see Fig. 9, the spectrum recorded at –0.6 V versus SCE in the presence of  $\text{O}_2$  is quite different from that at PNR-modified electrodes at the same potential owing to the more positive oxidation peak potential of PMG. The spectrum shows one semicircle with the beginning of a second one at low frequency. As in the case of PNR, the absence of oxygen leads to an increase in the impedance values, the film resistance increasing from 0.89 to 7.63  $\text{k}\Omega\text{ cm}^2$ . One obvious difference in the shape of the spectra can be seen, at –0.3 V versus SCE, when the second semicircle is replaced by a straight line at low frequencies in the absence of oxygen. The maximum value of film capacitance and minimum film resistance occurs at 0.0 V in the presence of oxygen, in the region of film oxidation/reduction.

PMB has very similar spectra to PMG, in terms of shape and impedance values, except at +0.3 V versus SCE. The low frequency diffusion component is still evident, the probable reason being the broad oxidation peak ends only at +0.6 V for PMB at pH 7. The film resistance decreases from 3.78  $\text{k}\Omega\text{ cm}^{-2}$  at –0.6 V versus SCE to 1.19  $\text{k}\Omega\text{ cm}^{-2}$  at –0.3 V versus SCE and then increases up to 9.57  $\text{k}\Omega\text{ cm}^{-2}$  at 0.3 V versus SCE, having the same tendency as in the case of PMG. As in the case of PMG, the capacitance value reaches a maximum value at 0.0 V versus SCE in the presence of oxygen, of 1.79  $\text{mF cm}^{-2}$ . In the absence of  $\text{O}_2$  one significant difference was observed, at –0.6 V versus SCE, when the curve assumes a more resistive semicircular profile for the film impedance, without the evidence of a second

interfacial process. In the frequency range tested, the curves maintained the same profile and the impedance values were almost the same. As in the presence of oxygen, the maximum film resistance, 16.7  $\text{k}\Omega\text{ cm}^{-2}$ , was at +0.3 V versus SCE.

The results show that at negative potentials there is oxygen diffusion through the polymer film, but, since there is evidence of diffusion even in the absence of oxygen, this means that other species also diffuse through the polymer matrix. This is in agreement with the cyclic voltammetry results. The polymers present different interfacial characteristics, PNR being significantly different from the other two. PNR characteristics are not significantly dependent on the presence of oxygen, in contrast to PMG and PMB, which at positive potentials, presented pronounced changes in the spectra profile and impedance values.

This information is extremely important for understanding the functioning of oxidase enzyme-based electrochemical enzyme biosensors which use oxygen as co-factor. The potential at which it is wished to use them is around 0.0 V in order to minimise interferences from other electroactive compounds in complex matrices. It has been seen that if positive potentials are employed with PMG and PMB films then the consumption of oxygen in the enzyme reaction will lead to increased resistance values of the mediator/enzyme films so that more negative potentials must be used to avoid this problem.

#### 4. Conclusions

The three phenazine monomers studied electropolymerise in different ways at carbon film electrodes, influenced by their chemical structures and thence the formation of the radical cation. Of the three, poly(neutral red) is shown to have the best adhesion at carbon film electrodes. It was observed that both  $\text{NO}_3^-$  and  $\text{SO}_4^{2-}$  anions had a catalytic effect on the electropolymerisation process and that PMG and PMB electropolymerise better in alkaline media.

Cyclic voltammetry showed that both anodic and cathodic peak currents depend linearly on the square root of the scan rate, implying diffusion-controlled processes which was shown to be due to diffusion of the counter cation. The electrolyte type influences the cyclic voltammogram shape and peak current, but does not have a significant influence on midpoint potential values and, in the pH range between 1 and 7, the formal potential values decrease linearly with increase in buffer pH.

The impedance spectra showed a response due to the polymer film matrix and to the polymer–solution interface, with diffusional characteristics, those of PMG and PMB being similar but different to those of PNR. The presence of dissolved oxygen in solution affects PNR spectra less than those of PMG and PMB. However, its influence on PMG and PMB properties is not significant at potentials close to 0.0 V versus SCE where these polymer films can be used as redox mediators, in electrochemical enzyme biosensors.

#### Acknowledgements

Financial support from Fundação para a Ciência e a Tecnologia (FCT), ICEMS (Research Unit 103), Portugal is

gratefully acknowledged. MMB and EMP thank FCT for PhD grants (SFRH/BD/27864/2006 and SFRH/BD/31483/2006 respectively).

## References

- [1] M.D. Insidies, R. John, P.J. Riley, G.G. Wallace, *Electroanalysis* 3 (1991) 879.
- [2] P.N. Bartlett, P. Tebbutt, C.H. Turrell, *Anal. Chem.* 64 (1992) 138.
- [3] M.E. Ghica, C.M.A. Brett, *Anal. Chim. Acta* 532 (2005) 145.
- [4] A.A. Karyakin, E.E. Karyakina, H.-L. Schmidt, *Electroanalysis* 11 (1999) 149.
- [5] A.A. Karyakin, E.E. Karyakina, W. Schuhmann, H.-L. Schmidt, *Electroanalysis* 11 (1999) 553.
- [6] A.A. Karyakin, E.E. Karyakina, W. Schuhmann, H.-L. Schmidt, *Electroanalysis* 6 (1994) 821.
- [7] A.A. Karyakin, O.A. Bobrova, E.E. Karyakina, *J. Electroanal. Chem.* 399 (1995) 179.
- [8] C.M.A. Brett, G. Inzelt, V. Kertesz, *Anal. Chim. Acta* 385 (1999) 119.
- [9] R. Yang, C. Ruan, J. Deng, *J. Appl. Electrochem.* 28 (1998) 1269.
- [10] C. Lei, J. Deng, *Anal. Chem.* 68 (1996) 3344.
- [11] B. Wang, S. Dong, *Talanta* 51 (2000) 565.
- [12] Y.V. Ulyanova, A.E. Blackwell, S.D. Minter, *Analyst* 131 (2006) 257.
- [13] M.E. Ghica, C.M.A. Brett, *Electroanalysis* 18 (2006) 748.
- [14] M.M. Barsan, C.M.A. Brett, *Talanta*, in press, doi:10.1016/j.talanta.2007.09.027.
- [15] M.M. Barsan, J. Klinčar, M. Baltic, C.M.A. Brett, *Talanta* 71 (2007) 893.
- [16] R. Pauliukaite, M.E. Ghica, M. Barsan, *J. Solid State Electrochem.* 11 (2007) 899.
- [17] C.A. Pessoa, Y. Gushikem, L.T. Kubota, L. Gorton, *J. Electroanal. Chem.* 431 (1997) 23.
- [18] F.D. Munteanu, L.T. Kubota, L. Gorton, *J. Electroanal. Chem.* 509 (2001) 2.
- [19] A. Arvand, S. Sohrabnezhad, M.F. Mousavi, M. Shamsipur, M.A. Zanchichi, *Anal. Chim. Acta* 491 (2003) 193.
- [20] D. Benito, J.J. García-Jereño, J. Navarro-Laboulais, F. Vicente, *J. Electroanal. Chem.* 446 (1998) 4.
- [21] M. Dubois, D. Billaud, *Electrochim. Acta* 47 (2002) 4459.
- [22] M. Dubois, G. Froyer, D. Billaud, *Spectrochim. Acta A* 60 (2004) 1831.
- [23] D. Benito, C. Gabrielli, J.J. García-Jereño, M. Keddad, H. Perrot, F. Vicente, *Electrochem. Commun.* 4 (2002) 613.
- [24] O.M.S. Filipe, C.M.A. Brett, *Electroanalysis* 16 (2004) 994.
- [25] M.E. Ghica, C.M.A. Brett, *Anal. Lett.* 39 (2006) 1527.
- [26] A.A. Karyakin, A.K. Strakhova, E.E. Karyakina, S.D. Varfolomeyev, *Bioelectrochem. Bioenerg.* 32 (1993) 35.
- [27] D.D. Schlereth, A.A. Karyakin, *J. Electroanal. Chem.* 395 (1995) 221.
- [28] C.M.A. Brett, A.M. Oliveira Brett, *Electrochemistry, Principles, Methods and Applications*, Oxford University Press, Oxford, 1993.
- [29] J. Hong, H. Ghourchian, S. Rezaei-Zarchi, A.A. Moosavi-Movahedi, S. Ahmadian, A.A. Saboury, *Anal. Lett.* 40 (2007) 483.
- [30] H. Liu, Y. Liu, J. Qian, T. Yu, J. Deng, *Talanta* 43 (1996) 111.
- [31] A. Heller, *J. Phys. Chem.* 96 (1992) 3579.
- [32] B. Persson, L. Gorton, *J. Electroanal. Chem.* 292 (1990) 115.
- [33] B. Persson, *J. Electroanal. Chem.* 287 (1990) 61.